

Title:
Proximodistal gradient in the perception of delayed stiffness

Authors:

Ilana Nisky¹, Pierre Baraduc², and Amir Karniel¹

Affiliation:

- 1) Department of Biomedical Engineering, Ben-Gurion university of the Negev, Beer-Sheva, Israel
- 2) Cognitive Neuroscience Centre, CNRS UMR5229/University of Lyon I, Bron, France

Contact information:

Amir Karniel, Biomedical Engineering Department, Ben-Gurion University of the Negev, POB 653, Beer-Sheva 84105, Israel, akarniel@bgu.ac.il, phone +97286479679 , fax +97286479628 .

Accepted for publication in the journal of neurophysiology March 25, 2010

Abstract:

Proximal and distal muscles are different in size, maximum force, mechanical action and neuromuscular control. In the current study we explore the perception of delayed stiffness when probing is executed using movement of different joints. We found a proximodistal gradient in the amount of underestimation of delayed stiffness in the transition between probing with shoulder, elbow, and wrist joints. Moreover, there was a similar gradient in the optimal weighting between estimation of stiffness and the inverse of estimation of compliance that predicted the perception of the subjects. These gradients could not be ascribed to differences in movement amplitude, duration, velocity, and force amplitude, as these variables were not significantly modulated by the joint used for probing. Mean force did not follow a similar gradient either. Therefore, we suggest that the observed gradient in perception reveals a proximodistal gradient in control, such that proximal joints are dominated by force control, whereas distal joints are dominated by position control.

Keywords: stiffness, compliance, delay, force control, position control

Introduction:

Our fingers are more dexterous than our shoulder, and our shoulder muscles stronger than finger muscles. The apparent biomechanical differences between limb segments are reflected in the distinct control of proximal versus distal joints. There are different control loops for distal and proximal muscles in the cerebellum and in reflex pathways (Kandel et al. 2000; Kurata and Tanji 1986). The corticospinal system has stronger influence over distal than proximal muscles (Brouwer and Ashby 1990; Lemon and Griffiths 2005; McKiernan et al. 1998; Palmer and Ashby 1992; Turton and Lemon 1999), whereas the reticular formation affects proximal muscles more potently than distal muscles (Davidson and Buford 2006; Riddle et al. 2009). A similar anatomical gradient is likely underlies the human proximodistal gradient in end point positional accuracy (Domenico and McCloskey 1987; Tan et al. 1994), perception of endpoint position accuracy (Hall and McCloskey 1983; Refshauge et al. 1995). According to these studies humans are more accurate in control and perception of the position of endpoint of the limb. Opposite gradients in maximum controllable force and resolution of force control were reported (Biggs and Srinivasan 2002; Hamilton et al. 2004; Tan et al. 1994); namely proximal joints are more successful in the control of force than distal. These could be also related to the reported gradient in muscle spindle density (Banks 2006; Buxton and Peck 1990). Lu et al. (Lu et al. 2000) showed that selective hemispheric anesthesia affected distal but not proximal proprioception of position. In agreement to this view, a proximodistal gradient was observed in the residual motor function after hemispherectomy (Dijkerman et al. 2008), stroke (Turton and Lemon 1999) and upper motor neuron lesions (Colebatch and Gandevia 1989). Here we asked whether a proximodistal gradient exists in the perception of delayed stiffness.

Recent studies explored the effect of a delay on perception of stiffness (Nisky et al. 2008; Pressman et al. 2007). It was found that subjects overestimated delayed stiffness and that overestimation increased monotonically with increasing delay. Furthermore, when the elastic field had a boundary (which is typically the case with actual objects), subjects tended to underestimate the stiffness if they stayed inside the field boundary, and overestimate it when they moved across the boundary (Nisky et al. 2008). These results were consistent with a model based on a linear combination between two estimation modes: 1) a regression of force-over-position, which predicts underestimation of delayed stiffness, and 2) a regression of position-over-force, which predicts overestimation of delayed stiffness. Nevertheless, the influence of the specific joints that were used for probing was not explored.

Recent evidence supports the notion that the distinction between force and position control, widely used in robotics (Raibert and Craig 1981), may be relevant for the human motor system. Independent motion and force control were explored recently (Chib et al. 2009; Venkadesan and Valero-Cuevas 2008), and sensory weighting between force and position cues was suggested (Mugge et al. 2009). We explained perception of delayed stiffness as combination of the concurrent operations of force and position control depending on the relative amount of interaction with the boundary of the force field (Nisky et al. 2008). We suggested that the estimation process was directly related to the control policy that guided the hand: force control implies estimation according to regression of position over force, yielding

overestimation of delayed stiffness, whereas position control implies estimation according to regression of force over position, yielding underestimation of delayed stiffness. If the weighting between the controllers across different joints is graded like the corticospinal termination pattern, a proximodistal gradient in delayed stiffness estimation should be observed.

The results reported here demonstrate that indeed there is a proximodistal gradient in estimation of delayed stiffness. This, together with converging evidence from the literature about difference in control of proximal versus distal joints, supports the view of a proximodistal gradient in combination of force and position control modes. Namely, proximal joints, such as shoulder and elbow, seem dominated by force control, whereas distal joints, such as wrist, seem dominated by position control. Part of this study was presented in recent conferences (Nisky and Karniel 2008; 2009).

Materials and methods:

Subjects, Apparatus and Protocol

Ten subjects participated in the experiments after signing the informed consent form as stipulated by the local Helsinki Committee. Subjects were seated and held with their dominant hand the handle of a PHANTOM® Desktop™ haptic device (SensAble Technologies, Inc.). They viewed through a semi-silvered horizontal mirror the virtual image of a CRT monitor (Reachin®/Sensegraphics® virtual reality system, figure 1a). An opaque screen was fixed under the glass to block the vision of the hand. Hand position was sampled through digital encoders in the haptic device at 77 Hz, and this information was used online to calculate the force feedback, which was interpolated and rendered at 1 kHz.

To investigate the perception of subjective stiffness, a forced-choice paradigm was used: in each trial, subjects were presented with two virtual elastic fields and were asked to choose which one of them was stiffer by probing both fields without time limits. One of the fields - the "D field" - had always a stiffness of 85 N/m, and its force feedback was delayed by 50 ms in half of the trials. The other – the "K field" – varied across trials: stiffness could be one of 10 equally spaced stiffness levels in the range of 40-130 N/m. The force feedback of the K field was never delayed. The delay of 50 ms is in the order of magnitude of the conduction delays to (and from) the muscles. In practice, this is large enough to be significant at typical probing velocities, and therefore to allow an observable distortion effects, but small enough to maintain a percept of stiffness. Subjects were instructed to make rapid probing movements and to keep the hand in motion. To avoid force saturation, subjects were asked to generate only short movements into the field, and a warning auditory cue sounded at the maximum allowed level of penetration (4.5 cm). After a short practice (during training trials), subjects learned to make short movements inside the allowed space. Subjects received only partial visual feedback of the probing hand location, only in directions perpendicular to the probing direction. They were instructed to make probing movements as straight as possible in the specified probing direction by minimizing the movement in these probing irrelevant directions as possible (see figure 1c-e for the directions of movement in the experiment). Each field was associated with a different background color (blue or red). Subjects were free to switch between the fields as often as they wished and to probe each field for as long as they wished. To switch between the two fields, subjects had to press a virtual button located in the right side of the working area, at $x = x_i$. Once they felt ready, they were asked to report which field was stiffer by pressing an appropriate button (blue or red) with the free nonprobing hand. The correspondence between the color (blue or red) and the field (K or D) as well as the order of presentation of the delayed field and the various levels of stiffness were all randomized; trials were presented in the same order to all the subjects. Each comparison of the K and D fields was considered as a single trial. The subjects performed 20 training trials and 200 test trials. Only the test trials were analyzed. Subjects were never provided with feedback about their answers.

We calculated the force feedback $F(t)$ exerted by the haptic device in order to emulate a spring-like field according to $F(t) = -K(x(t - \Delta t) - x_{0n})$, where K is the stiffness level,

$x(t)$ is the position of the robot handle along the probing direction (which will be specified further in text for different experimental conditions), Δt is the delay, and x_{0n} is the spring resting length (always unreachable, i.e., $x(t) > x_{0n}$). This ensured that the subject's hand remained inside the field and away from the boundary during the entire probing session in both delayed and nondelayed force fields. Accordingly, subjects always felt some nonzero force. This experimental setup is equivalent to probing stiffness while always maintaining contact with the probed object, similarly to abdominal palpation performed by a doctor during physical examination. To prevent discontinuity in the exerted force when subjects switched fields, the resting lengths, x_{0n} , were calculated such that $-K(x_i - x_{0n}) = F_i = -1N$. Subjects switched between the elastic fields by pressing a virtual button located at x_i ; therefore, they felt a force of 1 N, regardless of the stiffness level or the delay of the elastic field. Each subject repeated each experiment three times, in three different days, using different joints – wrist, elbow, and shoulder – to execute probing movements. Four subjects started the experiment in elbow condition, and six in wrist condition. We forced movement about specific joint using explicit instruction and splints, as depicted in figure 1c-e. For each joint we used a probing direction that was appropriate for the possible movement using that joint. These directions were similar

across subjects: $\hat{x} = \frac{\sqrt{2}}{2} \hat{j} - \frac{\sqrt{2}}{2} \hat{k}$ for wrist and elbow conditions, and

$\hat{x} = -\frac{\sqrt{2}}{2} \hat{j} - \frac{\sqrt{2}}{2} \hat{k}$ for shoulder condition, where $\hat{i}, \hat{j}, \hat{k}$ are unit vectors representing

apparatus x (right), y (forward), and z (up) directions. Subjects were instructed to avoid attempts to move around an irrelevant joint, and the splints prevented most of unintended movements. During the training trials the experimenter provided the subjects with general feedback about the probing movements and switching between force fields. At the end of the twenty training trials all subjects reported that they understood the task and they were comfortable with the probing movements and switching between fields. One of the subjects did not return to the lab to complete the experiment and was excluded from the data analysis.

Data Analysis

Psychometric curve

Psychometric curves were derived from the responses of the subjects in this force-choice task. We fitted the following equation to the data:

$$\psi(\Delta k, \alpha, \xi, \gamma, \lambda) = \gamma + (1 - \gamma - \lambda)S(\Delta k, \alpha, \xi)$$

where Δk is the intensity of the stimulus – the difference between the stiffness levels of the K and D fields. The shape of the curve is determined by the parameters: $[\alpha, \xi, \gamma, \lambda]$ and the choice of a two-parameter function S , typically a sigmoid. γ and λ are the rates of subjects' lapse – incorrect response regardless to the intensity of the difference between stiffness levels, and α and ξ determine the shift and the slope of the sigmoid function respectively. We used the psignifit toolbox version 2.5.6 for Matlab (Wichmann and Hill 2001b) to fit logistic function psychometric curves using a constrained maximum likelihood method for estimation of the parameters, and

found confidence intervals by the bias-corrected and accelerated (BC_a) bootstrap method described in (Wichmann and Hill 2001a).

We derived the psychometric function by estimating the subject's probability to answer "D is stiffer" as a function of the actual stiffness difference $\Delta K = K_D - K_K$, where K_D is the stiffness of the D field and K_K is the stiffness of the K field. This probability was calculated from the subject's answers according to:

$$P(\Delta K) = \frac{\sum_{n=1}^{N(\Delta K)} A[n]}{N(\Delta K)}; \quad A[n] = \begin{cases} 1 & D \text{ stiffer} \\ 0 & K \text{ stiffer} \end{cases}$$

where $A[n]$ is a binary representation of the subject's answer, and $N(\Delta K)$ is the total number of trials with stiffness difference ΔK .

Point of Subjective Equality (PSE)

After fitting the psychometric curve, we used the 0.5 threshold value of the logistic function to find the point of subjective equality (PSE), indicating the stiffness difference that was perceived to be zero. This amounts to assume that the error rate was independent of stiffness level (Wichmann and Hill 2001b). We expected PSE values close to 0 (unbiased stiffness estimation) for the nondelayed trials. For delayed trials, the psychometric curve was expected to shift. A positive PSE value would imply underestimation of delayed stiffness, since the delayed and nondelayed fields were perceived equal when the actual difference between their stiffness levels was positive. Similarly, negative PSE value would imply overestimation of delayed stiffness.

The slope of the psychometric curve at the PSE is a measure of the quality of discrimination between different stimulus levels. We estimated the slope by analytically calculating the gradient of the fitted psychometric function, namely

$$F'(x) \text{ at } x = F_{0.5}^{-1}.$$

Movement analysis

We recorded the position of the haptic device, and the force applied on the hand of the subject by the motors of the haptic device as a function of time during all probing time. A typical position trajectory fraction is depicted in figure 2. We analyzed the trajectories in the force-position space, i.e., a 2D space with one coordinate for the subject's hand position along the field direction (x) and one coordinate for the force exerted by the haptic device (F). For each trial we estimated the following parameters: **Mean probing movement period** - we automatically identified each probing movement according to local maxima and minima of the position trajectory (reversal points – solid and open circles in figure 2). Then we calculated number of probing movements in each trial, n_p , according to the number of local maxima, and calculated mean probing movement period $T_p = t_{\text{trial}}/n_p$, where t_{trial} is total probing time for the trial.

Mean probing movement amplitude – we calculated the difference between mean local maxima and minima of the position trajectory.

Mean absolute velocity – we considered only fingertip velocity along the field dimension (x); velocity was computed by numerical differentiation.

Mean peak absolute velocity – each probing movement consists of two submovements – the inward and outward movements. We identified peaks in absolute

velocity by finding the maximum absolute velocity for each submovement. Then we calculated the average of these peak absolute velocities.

Mean force amplitude – we calculated the difference between mean local maxima and minima of the force trajectory.

Mean absolute force – we calculated the average of absolute value of force exerted by the haptic device during the whole trial.

A last parameter was studied to assess the influence of trajectory curvature. Indeed, when motion is constrained to a single joint, hand paths are inevitably curved; in our study the extent of the probing movements was small relative to the radius of curvature in all three conditions, and this curvature is slight compared to the variance in execution of movement and movement of the robotic device relative to the hand of subjects. Nevertheless, we added to our movement analysis a measure that is a proxy to the curvature of movement in xy plane : the mean area reaching deviation (ARD) (Chib et al. 2006). From the definition below, one sees that straight paths with some noise yield zero ARD, whereas curved paths yields positive or negative ARD depending on the direction of curvature.

Mean area reaching deviation (ARD) – for each probing movement we identified the end point of movement as the point with largest distance from start point. Then we calculated the sum of the signed distances of all points to the straight line that connected start and end points of probing movement (which needs not to lie on the condition specific x axis), and divided by the total number of points.

Subjects were excluded from the analysis if their mean probing movement period across trials was found to be more than 500 ms in one of the conditions, since a slow probing movement essentially eliminates the effect of the delay. Two subjects were excluded from the analysis due to this criterion; we therefore present the results of seven subjects.

Optimal proximity index

We constructed a model that uses the trajectories of subjects in force-position space in order to predict their subjective judgment of which elastic fields are stiffer. Perception of stiffness is derived from information about force and position (Jones and Hunter 1990); however, the causality of force and position information in contact with elastic force field is not defined apriori, and it can be determined according the variable that is controlled by the motor system during contact. We can apply a certain force and measure the resultant displacement, or move the hand to a certain position inside the elastic field and measure the force. The stiffness of elastic force field can be estimated as a ratio between force and position, namely impedance; such estimation is appropriate if the subject controls position, and measures the force. However, stiffness can be also estimated as the inverse of compliance, a ratio between position and force, namely admittance; such estimation is appropriate if the controlled variable is the force applied by the subject, and the resultant penetration is measured. We propose a general class of models where the estimation of stiffness is based on a convex combination of these two estimations: stiffness (impedance) and the inverse of compliance (admittance), namely:

$$\hat{K} = (1 - \beta)\hat{K}_{stiffness} + \beta\hat{K}_{compliance}^{-1}.$$

The most important feature of our proposed model is the idea of combining estimation of stiffness and compliance, and not the exact model chosen to estimate either of them. Therefore, we compared the estimations according to two possible estimators of stiffness and compliance:

- 1) **Global regression based estimation:** $\hat{K}_{stiffness}$ is estimated according to the slope of regression of force over position, \hat{K}_{FP} , and $\hat{K}_{compliance^{-1}}$ is estimated according to the inverse of the slope of regression of position over force, \hat{K}_{PF} .
- 2) **Median of local numerical derivative in force-position plane:** $\hat{K}_{stiffness}$ is estimated according to median of local numerical differentiations of dF / dx , and $\hat{K}_{compliance^{-1}}$ is estimated according to the inverse of median of local numerical differentiations of dx / dF .

The model prediction of the subject's answer, $\hat{A}[n]$, was calculated according to the sign of the difference between estimations of D and K stiffness levels, \hat{K}_D and \hat{K}_K respectively, assuming an unbiased decision:

$$\hat{A}[n] = \begin{cases} 1 & \text{if } \hat{K}_D[n] - \hat{K}_K[n] > 0 \\ 0 & \text{if } \hat{K}_D[n] - \hat{K}_K[n] < 0 \end{cases}$$

While our models do not introduce any uncertainty that mimics the noise in the decision process of the subjects, there is some variability in the answers that are predicted by the model that reflects the variability in the actual probing movements. Therefore, psychometric curves were fitted to the predicted choices $\hat{A}[n]$. For each subject and for each probing joint condition we optimized the weight β in the range $[0, 1]$ to obtain the least possible squared difference between the actual and predicted psychometric curves. Thus, optimal β throughout this paper means optimal in the sense of best prediction of the experimental data.

Statistical analysis

We used repeated-measures one-way ANOVA (Glantz and Slinker 1990; Maxwell and Delaney 2004) in order to test the effect of joint condition on: (i) PSE in delayed trials, (ii) mean probing movement period, (iii) mean probing movement amplitude, (iv) mean absolute velocity, (v) mean peak absolute velocity, (vi) mean force amplitude, (vii) mean peak force, and (viii) mean ARD. We used Huynh-Feldt $\tilde{\epsilon}$ procedure to adjust for homogeneity assumption in repeated-measures ANOVA (Maxwell and Delaney 2004). We refer to p-values calculated using this adjustment as p_{adj} . We used the nonparametric Friedman's test (Friedman 1937) in order to test the effect of joint condition on optimal β , since β cannot be normally distributed (it is bounded in $[0,1]$). We used repeated-measures regression (ANCOVA) in order to test the relation between PSE in delayed trials and movement parameters (ii-viii), between PSE in delayed trials and optimal β , and between PSE of psychometric function fitted to models and subjects answers. Statistical significance was determined at the 0.05 level in all tests. We used `anovan` and `friedman` functions as implemented by MATLAB to perform the statistical analysis.

Control subsets analysis

In order to validate that some possible, even statistically not significant, gradients in movement period, amplitude, and force are not responsible for any gradient in PSE we performed analysis of subsets of trials in which these movement parameters were similar. For each subject we chose three different subsets of trials for analysis, such that movement periods, movement amplitudes, and movement force amplitudes were similar across joints in each of the subsets. These subsets are referred further as subset_i , where $i = \text{period, amplitude, or force}$ respectively. The trials that were included in the subsets were chosen according to the following procedure, which was repeated for each movement parameter i : (1) in each joint condition we calculated the mean parameter value for each test trial m_{ijk} , where $j = \text{wrist, elbow, shoulder}$ are the joint conditions, and $k = 21, \dots, 220$ are test trials numbers; (2) we found the first and ninety ninth percentiles m_{1ij} and m_{99ij} respectively, and calculated the minimal ninety ninth percentile, $\text{min}99_i = \min(m_{99ij})$, and maximal first percentiles, $\text{max}1_i = \max(m_{1ij})$; (3) we included in the subset only trials such that $\text{max}1_i < m_{ijk} < \text{min}99_i$. Then we fitted psychometric curves and extracted PSE values, taking only into account the answers of subjects from these subsets of trials.

Results:

Evidence for proximodistal gradient

The psychometric curves fitted to the performance of all seven subjects in the delayed trials revealed a significant proximodistal gradient in the perception of delayed stiffness when comparing probing with the shoulder joint to probing with the wrist joint. Figure 3a illustrates this for one subject in the shoulder (solid blue diamonds), elbow (dotted-dashed black squares), and wrist (dotted red circles) conditions: there was a positive gradient in the PSE in the transition from shoulder condition to wrist condition. Conversely as expected, this subject exhibited no bias in perceived stiffness or such effect of shift in the psychometric curves in non-delayed trials (figure 3a, light colors). This pattern was found in all subjects (figure 4a). Overall, the gradient in PSE values estimated from delayed trials was statistically significant (one-way ANOVA with repeated-measures $p=0.0002$, $p_{\text{adj}}=0.0005$, figure 4b). In contrast, it was not statistically different from zero for the nondelayed trials ($p=0.87$, figure 4b). There was a significant effect of delay ($p=0.004$) but not of joint ($p=0.34$) and no interaction between delay and joint ($p=0.83$) on the slopes of psychometric curves. These results indicate: 1) unbiased estimation of nondelayed stiffness when using any of the three joints, and 2) stronger underestimation of delayed stiffness when subjects used their wrist than when they used their elbow to probe the force field, and weaker underestimation (and sometimes overestimation) when they used their shoulder. These results are consistent with our hypothesis of a proximodistal gradient in the ratio of force control to position control.

Proximity index gradient indicates proximodistal gradient in force-position control

Figure 3b depicts force-position trajectories in wrist (red circles), elbow (black squares), and shoulder (blue diamonds) conditions for the same trial number of one subject. The trajectories are qualitatively similar, and it is clear that delay had substantial effect on all three trajectories, which would otherwise be similar to straight lines in the force-position plane. There was no statistically significant effect of the probing joint on mean probing movement period, amplitude, absolute velocity, absolute peak velocity, force amplitude, and mean ARD (see figure 5 and table 1). There was a statistically significant effect of probing joint on mean absolute force, but there was no proximodistal gradient (figure 5). In order to test whether a gradient in any of the movement parameters can explain the gradient in perception we performed a repeated-measures regression between PSE and these parameters and found that the slope was not significantly different from zero for any of the parameters (see table 1). To further validate that the apparent nonsignificant gradients in movement period, amplitude, and force were not responsible for the proximodistal gradient in PSE that we observed, we repeated the analysis in a way that created control datasets for these parameters. We still found a statistically significant proximodistal gradient (ANOVA with repeated measures $p<0.0001$ for $\text{subset}_{\text{period}}$, $p=0.003$ for $\text{subset}_{\text{amplitude}}$, and $p=0.0009$ for $\text{subset}_{\text{force}}$). Altogether this analysis rules out the possibility that the observed estimation differences simply reflect kinematic differences between the movements.

We found a statistically significant gradient in the optimal values of β from probing with the wrist to probing with the shoulder for both methods of estimation of stiffness

and compliance (Friedman test, $p=0.032$ for regression based estimation, and $p=0.012$ for median of local numerical derivatives), as depicted in figure 6 a-b. Moreover, repeated-measures regression between PSE and optimal β yielded a slope significantly different from zero for both methods of estimation (see table 1), further strengthening the connection between gradient in proximity index and in perception of delayed stiffness.

In order to assess the ability of the suggested models to predict the answers of subjects, we fitted a regression line between PSE that were extracted from the model prediction and PSE that were extracted from subjects' answers. An ideal model is expected to yield a zero intercept and a unity slope. The performance of models that use estimation of stiffness only is depicted in figure 6 c-d, whereas the performance of models which combine estimation of stiffness with the inverse of estimation of compliance is depicted in figure 6 e-f. Statistical analysis of the regression is summarized in table 2. One can clearly see that adding weighting between estimation of impedance (stiffness) and the inverse of the estimation of admittance (compliance) is essential in order to account for the subjects' answers, regardless of the particular model that was used for each of the estimations. It should be emphasized that the good fit here is not a direct result of the optimization process: the weighted components are two specific estimates of stiffness; moreover, since $\beta \in [0,1]$ the combined model can only yield estimations that are between the estimations as impedance and the inverse of admittance. For example, if the position-over-force regression predicted overestimation, and force-over-position predicted no change in perception, there would still be a gradient in the optimal β , but the fit of the regression with the PSE would be rather poor. Thus, the good fit supports the hypothesis of a combined model for the perception of stiffness. This analysis, taken together with the statistically significant gradient in the optimal values of β (as depicted in figure 6a-b) further supports the hypothesis that the proximodistal gradient in perception is related to a proximodistal gradient in control.

Parameter	ANOVA with repeated measures		Regression with repeated measures	
	P	p _{adj}	slope	p
Probing movement period	0.35	0.34	2.52 [Nm ⁻¹ s ⁻¹]	0.96
Probing movement amplitude	0.14	0.14	-12 [Nm ⁻¹ cm ⁻¹]	0.12
Absolute velocity	0.27	0.27	-19 [Nsm ⁻²]	0.87
Peak absolute velocity	0.9	0.94	28 [Nsm ⁻²]	0.67
Force amplitude	0.18	0.18	-13 [m ⁻¹]	0.18
Absolute force	0.047	0.047	-17 [m ⁻¹]	0.24
Mean ARD	0.23	0.24	-22 [Nm ⁻¹ cm ⁻¹]	0.84
Optimal β	Friedman's test			
Regression based model	0.032	-	-28 [N/m]	0.013
Local derivative based model	0.012	-	-52 [N/m]	0.005

Table 1: Summary of statistical analysis of movement parameters and optimal β . In bold are p values for statistically significant tests at the 0.05 significance level.

Model	Global regression based				Local derivatives based			
	int.	sl.	p	r ²	int.	sl.	p	r ²
$\hat{K} = \hat{K}_{stiffness}$	15	0.45	0.01	0.27	45	0.06	0.59	0.01
$\hat{K} = \beta \hat{K}_{stiffness} + (1 - \beta) \hat{K}_{compliance^{-1}}$	-1	0.91	<0.0001	0.86	-1.8	1.27	<0.0001	0.87

Table 2: Comparison between the prediction of the models and the answers of the subjects. The ideal model is expected to yield zero intercept (int.) and unity slope (sl.). Weighted models are clearly superior to models that merely use estimation of stiffness in all aspects of the regression analysis.

Discussion:

In this study we report the existence of a proximodistal gradient in the perception of delayed stiffness. There was a statistically significant proximodistal gradient in the extent of stiffness underestimation in the transition from probing with the shoulder to probing with the wrist. In models that combine estimations of stiffness and inverse of compliance the optimal mixing weight was significantly graded along a proximodistal axis. In contrast, we found no statistically significant effect of joint on the extent, duration, velocity, or force amplitude of probing movements, indicating that the observed perceptual gradient is not the result of differences in movement kinematics.

The gradient reported here is not in the absolute sensitivity to the delay, but in the amount of underestimation; namely, the gradient is in the signed value of the difference between perceived stiffness and actual stiffness. Depending on the subject, we observed a transition from overestimation to correct estimation, from correct estimation to underestimation, and from underestimation to stronger underestimation. Therefore, the gradient in perception of delayed stiffness cannot be explained as a simple consequence of the relative size of delay when compared to the neural delay of information transfer to a specific joint.

This study continues our previous studies of the effect of delay on perception of the stiffness of elastic force fields (Nisky et al. 2008; Pressman et al. 2007). The stiffness of such a field is the ratio between the applied force and penetration. In the non-delayed case, the trajectory in force position space is a straight line. However, introducing delay between the penetration and the applied force causes this trajectory to become elliptical, the force is no longer a single valued function of position, and during a single probing movement, the local stiffness is some times lower and at other times higher than the non delayed stiffness. The present results confirm that the global stiffness percept is a mixture of these local estimates and demonstrates that it is modulated by the nature of the limb segment moved.

The force position trajectory of nearly periodic, sinusoidal, probing movements during interaction with delayed elastic force field could resemble the trajectory of a viscoelastic time-independent force field. Therefore it is interesting to explore whether the perceptual effects of delay that we observed in this study are the result of the viscosity in such approximated force field. The discrimination of viscosity was studied extensively (Beauregard et al. 1995; Jones and Hunter 1993; Nicholson et al. 2003), and it was reported that the Weber fraction for perception of viscosity is much larger than for perception of stiffness. However, further research is required in order to map the effect of viscosity on stiffness estimation and consider the possible similarities to the perception of delayed elastic field.

In our previous studies, we found that subjects tend to overestimate delayed stiffness when they move across the field boundary, and underestimate it if they do not cross the boundary (Nisky et al. 2008; Pressman et al. 2007). A model based on a convex combination between the slope of regression of force-over-position (implying position control) and the inverse of the slope of position-over-force (implying force control) regression according to the relative fraction of probing movements completed outside and inside the field best predicted the behavioral results. Here we extended that model in order to include the influence of a proximity index on the weighting between force and position control. Subjects did not have access to the boundary; however, the

optimal weighting parameter β was not zero. Moreover, there was a distal to proximal gradient in optimal β in the transition between different probing joints, regardless to the specific model that was used for estimation of stiffness and compliance, and therefore we refer to the weighting parameter β as proximity index. We suggest that there is a proximodistal gradient in control: proximal joints are dominated by combination of force and position control ($\beta \approx 0.5$), whereas distal joints are dominated by position control ($\beta \approx 0.1$). For the purpose of illustrating the possible role of such a gradient in control, consider an everyday scenario of inserting a key into a keyhole while holding a heavy grocery bag. To succeed in such a task, one needs to precisely control the position (angles) of the digits and wrist in order to aim the key at the keyhole, and precisely compensate for gravitational forces at the shoulder in order to maintain stable posture.

In this study we used two different estimators for the relation between position and force and the reciprocal relation between force and position: the slope of a regression, and median of local derivatives in force position plane. Our analysis was not sensitive to the choice of the particular estimator (compare planes a-c-e and b-d-f in figure 6), and other estimators can be suggested. We presented analysis of both models in order to emphasize that the important issue here is the combination of estimation of stiffness with the inverse of estimation of the compliance, and not the exact model for estimating either of them.

Our general hypothesis is that position and force control operate concurrently in the motor system, and are weighted according to demands opposed by the environment, such as boundary crossing, as well as according to the proximity of the joint that is involved in the probing movement. The weight of force control is increased with increasing boundary crossing ratio and with the proximity of the probing joint. Consequently, the perceived stiffness in such a system is a weighting between estimation of stiffness (impedance), which yields overestimation, and inverse of estimation of compliance (admittance), which yields underestimation. Therefore, a proximodistal gradient in underestimation of delayed stiffness, as well as transition between underestimation and overestimation of delayed stiffness according to the boundary crossing ratio are observed.

There is a recent accumulation of evidence supporting independent force and position control in the motor system (Chib et al. 2009; Venkadesan and Valero-Cuevas 2008). A similar framework can be used to explain why an increase in environment stiffness caused transition from restoring unperturbed trajectory to compliance with the perceived object boundary (Chib et al. 2006): position control is weighted stronger at low levels of stiffness, and therefore the unperturbed trajectory is restored; force control dominates in contact with high level of stiffness, and therefore the perceived "object" boundary is followed while maintaining constant interface force. Such weighting is consistent with sensory weighting between force and position cues when handling soft elastic objects (Mugge et al. 2009), where the weight of the force increases with the level of stiffness, and the weight of the position decreases accordingly. The weights of position and force in estimation could be determined by the weights of the appropriate modes in control. Our results are consistent with (Mugge et al. 2009): we however probed a much narrower range of stiffness levels,

and therefore could not observe a similar effect of field stiffness level on weighting between force and position control modes. Moreover, our results about the gradient in control between different probing joints might be the underlying reason for the large variability in the experimental data at 100N/m stiffness level presented in (Mugge et al. 2009).

There is ample evidence for differences in the control and representation of proximal versus distal joints throughout the nervous system. There is a widely accepted division in control responsibility over distal and proximal muscles between the corticospinal and the reticulospinal tracts (Brouwer and Ashby 1990; Davidson and Buford 2006; Lemon and Griffiths 2005; McKiernan et al. 1998; Palmer and Ashby 1992; Turton and Lemon 1999). New studies question this picture (Riddle et al. 2009), but although human studies showed that there are monosynaptic corticomotoneuronal projections to proximal arm muscles (Colebatch et al. 1990), these are bilateral rather than unilateral as the projections to distal muscles. Moreover, in primates, the projections to distal muscles are stronger and more potent than to proximal muscles (Brouwer and Ashby 1990; Lemon and Griffiths 2005; Palmer and Ashby 1992; Turton and Lemon 1999). While in the recent decades the idea of somatotopic organization of the motor cortex is questioned (Schieber 2001) a general segregation between representations of proximal and distal muscles is evident in the motor (Asanuma and Rosén 1972; Schieber 2001) and premotor cortex (Freund and Hummelsheim 1984; Kurata and Tanji 1986). In addition, the magnocellular red nucleus was shown to have stronger influence on distal than on proximal muscles (Belhaj-Saif et al. 1998; Houk et al. 1988; Lawrence and Kuypers 1968; Miller et al. 1993; Ralston et al. 1988). Proximodistal gradient was also observed in the control of avian running (Daley et al. 2007), in reflex responses of squirrel monkey (Lenz et al. 1983), and in human motor performance and perception (Domenico and McCloskey 1987; Gandevia and Kilbreath 1990; Hall and McCloskey 1983; Hamilton et al. 2004; Refshauge et al. 1995; Tan et al. 1994).

In the conceptual framework that we lay out in this paper there is rather speculative leap between the behavioral results and the possible underlying weighting between force and position control in the neural control of movement. The percept of stiffness we measured reflects how force and position feedback are integrated to produce a coherent picture of the attributes of the manipulated object. We here hypothesize that variation of this integrative process with the nature of the joint used is likely accompanied by a similar variation in the sensorimotor control — since the latter is based on the same afferent signals. Indeed, the proximodistal gradient in perception and in weighting between force and position control suggested in this study is in line with the neurophysiological evidence reviewed above, which concerns the perceptual as well as the control aspects of sensorimotor function. This agreement gives some credit to our proposed connection between perception and control (Nisky et al. 2008). However, we readily acknowledge that we did not provide here a direct evidence for combination of force and position control in the control of explorative movements in contact with elastic force fields. These, as well as the exact neuromechanical processes underlying our new observation of a proximodistal gradient in the perception of delayed stiffness remain open for future studies.

Grants:

This research was supported by a grant from the Ministry of Science, Culture & Sport, Israel & the Ministry of Research, France, as well as by a grant from the Israel United State Binational Science Foundation (BSF). IN is supported by the Kreitman foundation and the Clore Scholarship Program.

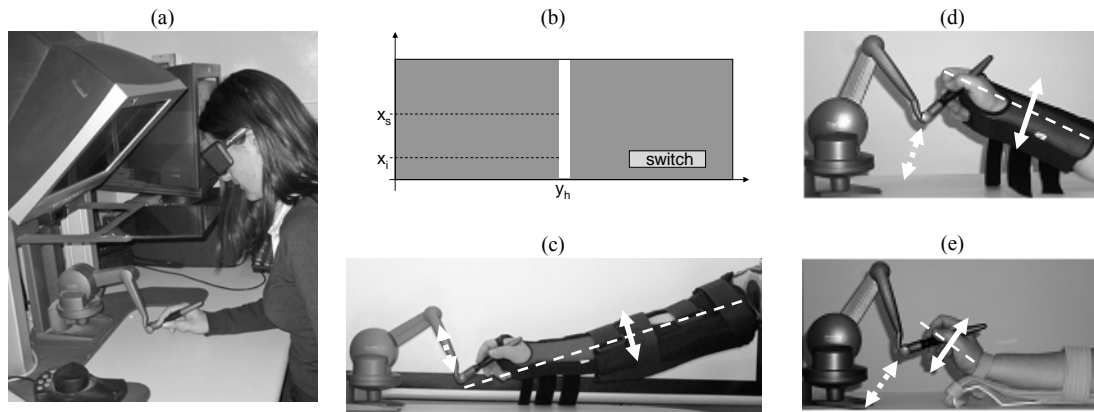


Figure 1: Experimental setup: (a) The subject and the virtual reality system. (b) The view presented to subject at each trial: the direction of probing is x ; gray rectangle represents blue/red elastic force field; white rectangle represents partial feedback about hand location, in directions perpendicular to the direction of probing; switch rectangle represents the virtual button that subjects pressed in order to switch between different fields in the same trial; x_s is the location where the auditory warning was sounded. (c)-(e) Illustrations of the three movement conditions: shoulder movement (c), elbow movement (d), and wrist movement (e). Solid white arrows show the direction of probing movement. Dashed white arrows show the direction of haptic device endpoint movement during probing. The position of this endpoint determines the force that the haptic device applies on the hand of the subject. Dashed white lines show the main axis of the moving part of the forelimb: (c) arm, (d) forearm, (e) hand.

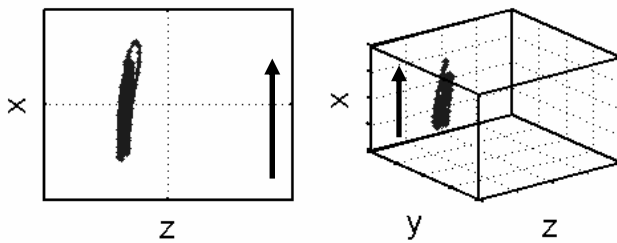
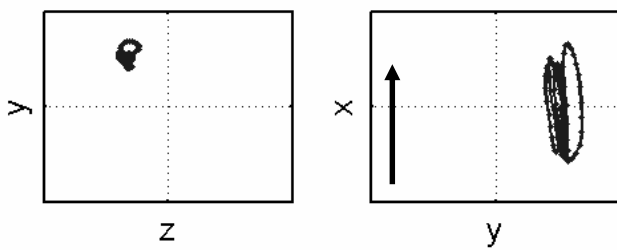
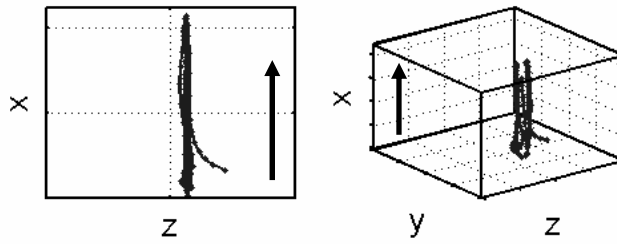
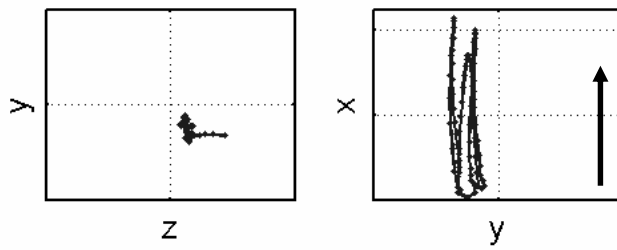
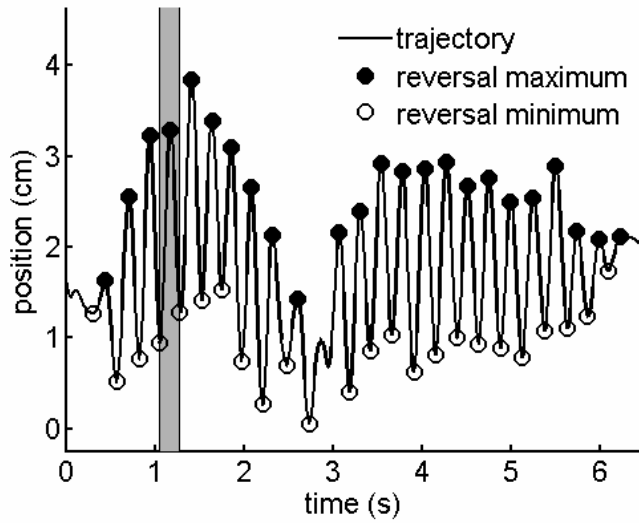
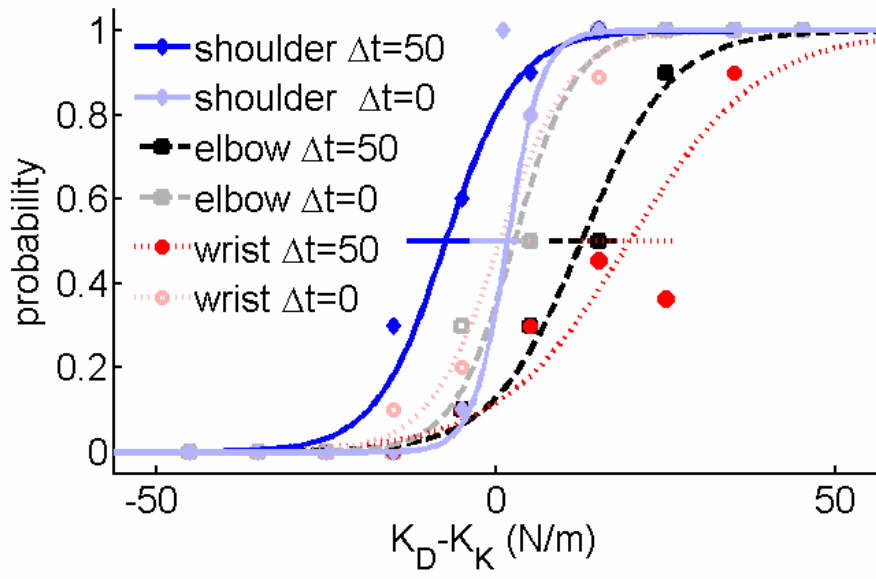
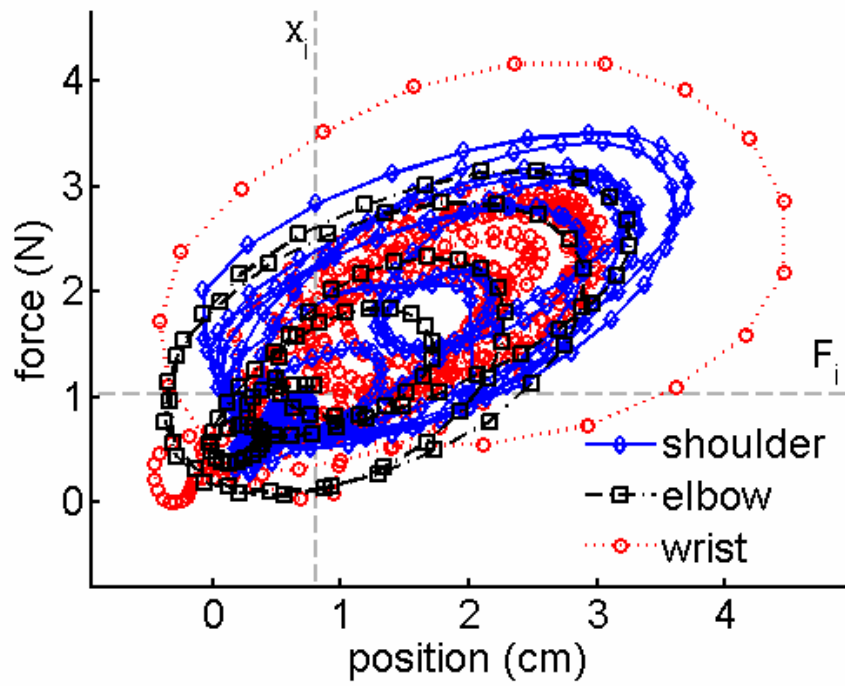


Figure 2: (a) An example of a position trajectory from a single trial of a single subject as a function of probing time. Solid and open circles indicate local maxima and minima respectively. Shaded area highlights a single probing movement. The local extrema were identified in temporal windows of 100ms. In addition we required at least 1mm spatial difference between adjacent minima and maxima. (b)-(c) Examples of probing movements position data including off (y,z) and on (x) axis movements in shoulder (b) and wrist (c) conditions. Arrows show direction of elastic force field. Each tick of grids is 1cm.

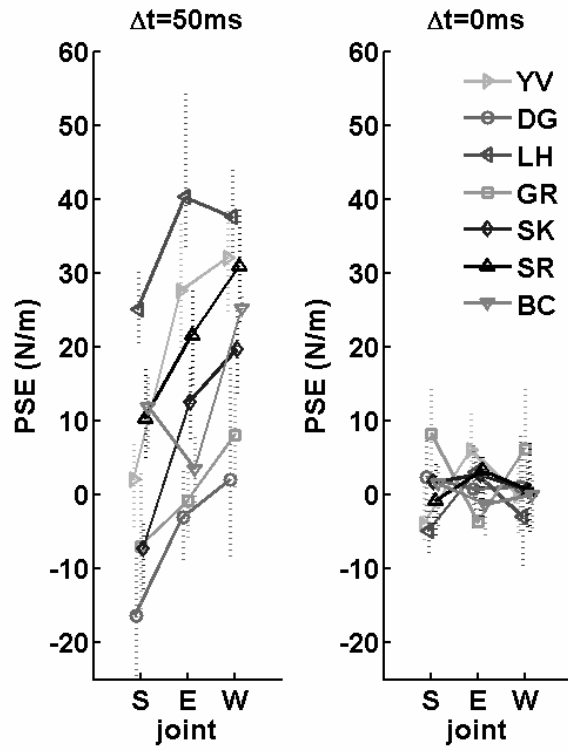


(a)

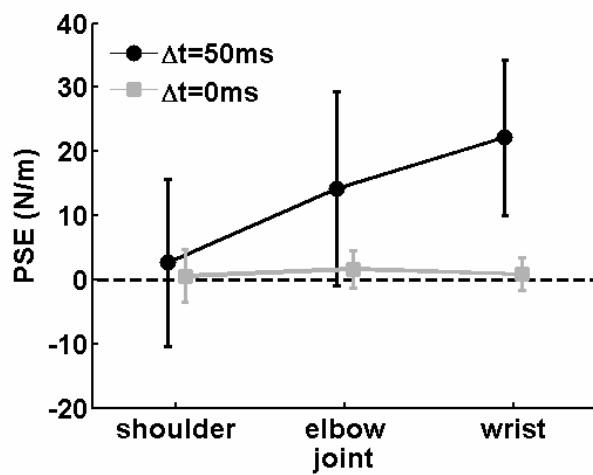


(b)

Figure 3: Results of a single subject (SK) in shoulder (solid blue line and diamond marker), elbow (dashed-dotted black line and square marker), and wrist (dotted red line and circle marker) conditions. (a) Psychometric curves fitted according to answers in delayed (darker symbols and lines) and nondelayed (lighter symbols and lines) trials. Horizontal error bars are 95% confidence intervals for the estimation of the PSE. In non-delayed trials the probability to answer "D stiffer" changes from zero to one around null difference between D and K force fields, whereas the curves fitted to answers in delayed trials are shifted to left (shoulder) or right (elbow and wrist), indicating this subject's overestimation or underestimation of delayed stiffness respectively. The curve describing answers in the "wrist" condition is shifted further to the right than in the "elbow" condition. (b) Force-position trajectories from similar trials in all three conditions. Trajectories are ellipsoid due to the effect of delay. There is no qualitative difference between the forms of the trajectories.



(a)



(b)

Figure 4: Proximodistal gradient in the change in perception of stiffness caused by delay revealed when subjects probe the force field with their shoulder, elbow, and wrist. (a) Left and right panels depict individual PSE values in delayed and nondelayed conditions respectively. Subject symbols coding is common to both panels. Markers are estimates of PSE, and dotted bars are 95% confidence intervals on these estimates of PSE. In the delayed condition, the PSE values increase in the transition between shoulder (S), elbow (E), and wrist (W). Note that the slope of the gradient is similar in all subjects, but that the intercept (amount of under- or over-estimation) is subject-dependent. In contrast, in the nondelayed (control) condition all PSE values cluster around zero for all subjects, indicating no bias in estimation of stiffness whatever joint is used. (b) Mean PSE values across all subjects for delayed (black circles) and nondelayed (gray squares) trials. Markers are mean PSE and error bars are 95% confidence intervals for the mean PSE. The gradient in mean PSE is statistically significant (see Results).

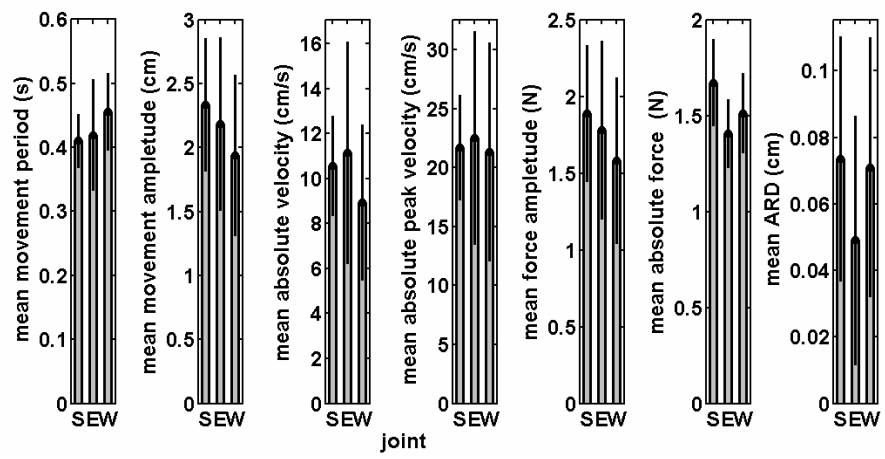


Figure 5: Absence of statistically significant effect of probing joint on mean movement period, movement amplitude, absolute velocity, peak absolute velocity, force amplitude, and ARD, and significant effect of joint without proximodistal gradient on mean absolute force. The presented data is for shoulder (S), elbow (E), and wrist (W) motion. Bars are the mean, and error bars are 95% confidence intervals for the estimation of the mean in each plot. See text for details on the statistical analysis.

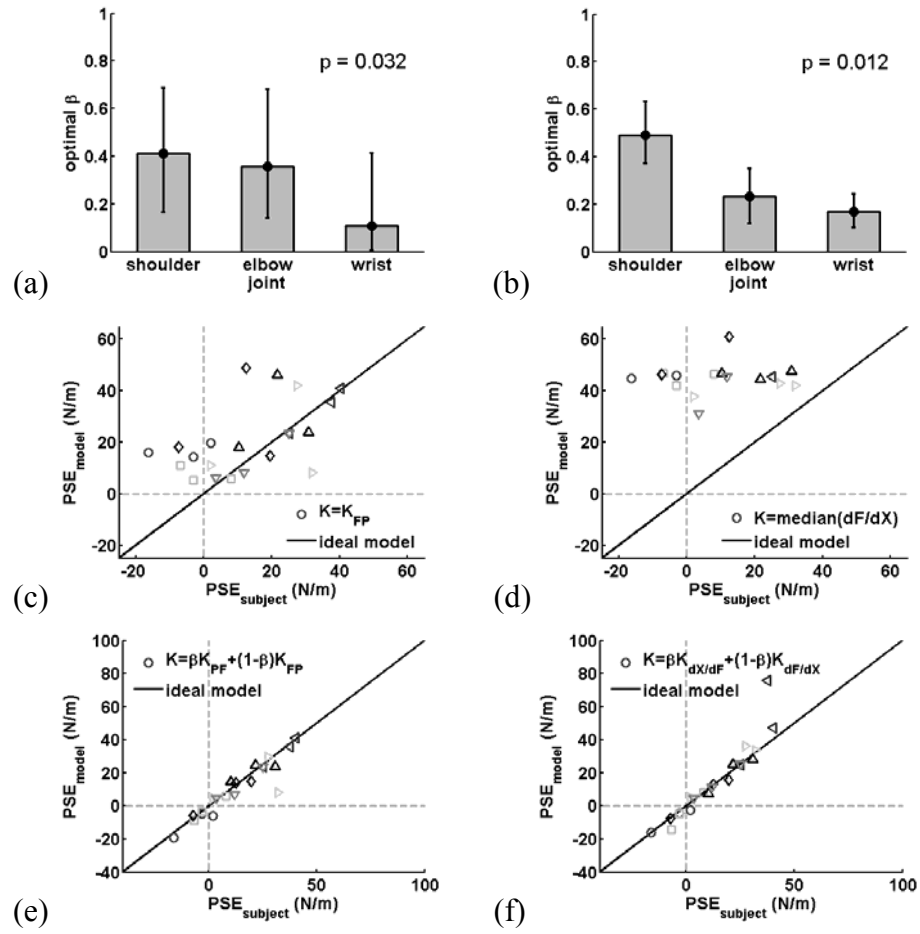


Figure 6: Model comparison. In (a), (c), (e) models are based on regression in force-position plane. In (b), (d), (f) models are based on median of local numerical derivatives. (a)-(b) Effect of probing joint on the optimal β . Bars are the mean, and error bars are 95% confidence intervals for the estimation of the mean in each plot. The optimal β is significantly modulated by the joint that was used for probing. (c)-(f) Comparison between models and subject answers. The solid black line describes the ideal model. Symbols coding as in figure 2. (c)-(d) Models were based on estimation of stiffness. (e)-(f) Models were based on a combination between estimation of stiffness and the inverse of estimation of compliance. Each subject is represented by a unique symbol; symbol coding is similar to Figure 4.

- Asanuma H, and Rosén I.** Topographical organization of cortical efferent zones projecting to distal forelimb muscles in the monkey. *Experimental Brain Research* 14: 243-256, 1972.
- Banks RW.** An allometric analysis of the number of muscle spindles in mammalian skeletal muscles. *Journal of Anatomy* 208: 753-768, 2006.
- Beauregard GL, Srinivasan MA, and Durlach NI.** The manual resolution of viscosity and mass. In: *ASME Dynamic Systems and Control Division 1995 IMECE1995*, p. 657-662.
- Belhaj-Saif A, Karrer JH, and Cheney PD.** Distribution and Characteristics of Poststimulus Effects in Proximal and Distal Forelimb Muscles From Red Nucleus in the Monkey. *Journal of Neurophysiology* 79: 1777-1789, 1998.
- Biggs J, and Srinivasan MA.** Haptic Interfaces. In: *Handbook of Virtual Environments*, edited by Stanney K. London: Lawrence Earlbaum, Inc, 2002, p. 93-115.
- Brouwer B, and Ashby P.** Corticospinal projections to upper and lower limb spinal motoneurons in man. *Electroencephalogr Clin Neurophysiol* 76: 509-519, 1990.
- Buxton DF, and Peck D.** Density of muscle spindle profiles in the intrinsic forelimb muscles of the dog. *Journal of Morphology* 203: 345-359, 1990.
- Chib VS, Krutky MA, Lynch KM, and Mussa-Ivaldi FA.** The Separate Neural Control of Hand Movements and Contact Forces. *J Neurosci* 29: 3939-3947, 2009.
- Chib VS, Patton JL, Lynch KM, and Mussa-Ivaldi FA.** Haptic Identification of Surfaces as Fields of Force. *J Neurophysiol* 95: 1068-1077, 2006.
- Colebatch JG, and Gandevia SC.** The distribution of muscular weakness in upper motor neuron lesions affecting the arm. *Brain* 112: 749-763, 1989.
- Colebatch JG, Rothwell JC, Day BL, Thompson PD, and Marsden CD.** CORTICAL OUTFLOW TO PROXIMAL ARM MUSCLES IN MAN. *Brain* 113: 1843-1856, 1990.
- Daley MA, Felix G, and Biewener AA.** Running stability is enhanced by a proximo-distal gradient in joint neuromechanical control. *Journal of experimental biology* 210: 383-394, 2007.
- Davidson A, and Buford J.** Bilateral actions of the reticulospinal tract on arm and shoulder muscles in the monkey: stimulus triggered averaging. *Experimental Brain Research* 173: 25-39, 2006.
- Dijkerman HC, Vargha-Khadem F, Polkey CE, and Weiskrantz L.** Ipsilesional and contralesional sensorimotor function after hemispherectomy: Differences between distal and proximal function. *Neuropsychologia* 46: 886-901, 2008.
- Domenico G, and McCloskey DI.** Accuracy of voluntary movements at the thumb and elbow joints. *Experimental Brain Research* 65: 471-478, 1987.
- Freund HJ, and Hummelsheim H.** Premotor cortex in man: Evidence for innervation of proximal limb muscles. *Experimental Brain Research* 53: 479-482, 1984.
- Friedman M.** The Use of Ranks to Avoid the Assumption of Normality Implicit in the Analysis of Variance. *Journal of the American Statistical Association* 32: 675-701, 1937.
- Gandevia SC, and Kilbreath SL.** Accuracy of weight estimation for weights lifted by proximal and distal muscles of the human upper limb. *Journal of Physiology* 423: 299-310, 1990.
- Glantz SA, and Slinker BK.** *Primer of applied regression and analysis of variance*. New York: McGraw-Hill 1990.
- Hall LA, and McCloskey DI.** Detections of movements imposed on finger, elbow and shoulder joints. *The Journal of Physiology* 335: 519-533, 1983.
- Hamilton AF, Jones KE, and Wolpert DM.** The scaling of motor noise with muscle strength and motor unit number in humans. *Experimental Brain Research* 157: 417-430, 2004.

- Houk JC, Gibson AR, Harvey CF, Kennedy PR, and van Kan PLE.** Activity of primate magnocellular red nucleus related to hand and finger movements. *Behavioural Brain Research* 28: 201-206, 1988.
- Jones LA, and Hunter IW.** A perceptual analysis of stiffness. *Exp Brain Res* 79: 150-156, 1990.
- Jones LA, and Hunter IW.** A perceptual analysis of viscosity. *Experimental Brain Research* 94: 343-351, 1993.
- Kandel E, Schwartz J, and Jessel T.** *Principles of neural science* McGraw-Hill, 2000.
- Kurata K, and Tanji J.** Premotor cortex neurons in macaques: activity before distal and proximal forelimb movements. *Journal of Neuroscience* 6: 403-411, 1986.
- Lawrence DG, and Kuypers HGJM.** THE FUNCTIONAL ORGANIZATION OF THE MOTOR SYSTEM IN THE MONKEY: II. THE EFFECTS OF LESIONS OF THE DESCENDING BRAIN-STEM PATHWAYS. *Brain* 91: 15-36, 1968.
- Lemon RN, and Griffiths J.** Comparing the function of the corticospinal system in different species: Organizational differences for motor specialization? *Muscle & Nerve* 32: 261-279, 2005.
- Lenz FA, Tatton WG, and Tasker RR.** Electromyographic response to displacement of different forelimb joints in the squirrel monkey. *Journal of Neuroscience* 3: 783-794, 1983.
- Lu LH, Barrett AM, Cibula JE, Gilmore RL, and Heilman KM.** Proprioception more impaired distally than proximally in subjects with hemispheric dysfunction. *Neurology* 55: 596-597, 2000.
- Maxwell SE, and Delaney HD.** *Designing Experiments and Analyzing Data: A Model Comparison Perspective.* Mahwah, New Jersey: Lawrence Erlbaum Associates, 2004.
- McKiernan BJ, Marcario JK, Karrer JH, and Cheney PD.** Corticomotoneuronal Postspike Effects in Shoulder, Elbow, Wrist, Digit, and Intrinsic Hand Muscles During a Reach and Prehension Task. *J Neurophysiol* 80: 1961-1980, 1998.
- Miller LE, van Kan PL, Sinkjaer T, Andersen T, Harris GD, and Houk JC.** Correlation of primate red nucleus discharge with muscle activity during free-form arm movements. *The Journal of Physiology* 469: 213-243, 1993.
- Mugge W, Schuurmans J, Schouten AC, and van der Helm FCT.** Sensory Weighting of Force and Position Feedback in Human Motor Control Tasks. *Journal of Neuroscience* 29: 5476-5482, 2009.
- Nicholson LL, Adams RD, and Maher CG.** Manual discrimination capability when only viscosity is varied in viscoelastic stiffness stimuli. *Journal of Manipulative and Physiological Therapeutics* 26: 365-373, 2003.
- Nisky I, and Karniel A.** Does the brain use force or position control when probing the stiffness of virtual elastic force fields? In: *Program No 46514 2008 Neuroscience Meeting Planner, Society for Neuroscience, 2008 Online.* Washington, DC: 2008.
- Nisky I, and Karniel A.** Proximodistal gradient in the perception of delayed stiffness. In: *Virtual Rehabilitation 2009.* Haifa, Israel: 2009.
- Nisky I, Mussa-Ivaldi FA, and Karniel A.** A Regression and Boundary-Crossing-Based Model for the Perception of Delayed Stiffness. *Haptics, IEEE Transactions on* 1: 73-82, 2008.
- Palmer E, and Ashby P.** Corticospinal projections to upper limb motoneurons in humans. *J Physiol* 448: 397-412, 1992.
- Pressman A, Welty LH, Karniel A, and Mussa-Ivaldi FA.** Perception of delayed stiffness. *The international Journal of Robotics Research* 26: 1191-1203, 2007.
- Raibert MH, and Craig JJ.** Hybrid position/force control of manipulators. *ASME journal of dynamic systems, measurement, and control* 102: 126-133, 1981.

Ralston DD, Milroy AM, and Holstege G. Ultrastructural evidence for direct monosynaptic rubrospinal connections to motoneurons in *Macaca mulatta*. *Neuroscience Letters* 95: 102, 1988.

Refshauge KM, Chan R, Taylor JL, and McCloskey DI. Detection of movements imposed on human hip, knee, ankle and toe joints. *The Journal of Physiology* 488: 231-241, 1995.

Riddle CN, Edgley SA, and Baker SN. Direct and Indirect Connections with Upper Limb Motoneurons from the Primate Reticulospinal Tract. *Journal of Neuroscience* 29: 4993-4999, 2009.

Schieber MH. Constraints on Somatotopic Organization in the Primary Motor Cortex. *Journal of Neurophysiology* 86: 2125-2143, 2001.

Tan HZ, Srinivassan MA, Eberman B, and Cheng B. Human factors for the design of force reflecting haptic interfaces In: *DSC Dynamic Systems and Control (The American Society of Mechanical Engineers)*, edited by Radcliffe CJ1994.

Turton A, and Lemon RN. The contribution of fast corticospinal input to the voluntary activation of proximal muscles in normal subjects and in stroke patients. *Experimental Brain Research* 129: 559-572, 1999.

Venkadesan M, and Valero-Cuevas FJ. Neural Control of Motion-to-Force Transitions with the Fingertip. *J Neurosci* 28: 1366-1373, 2008.

Wichmann FA, and Hill NJ. The psychometric function: I. Fitting, sampling, and goodness of fit. *Percept Psychophys* 63: 1293-1313, 2001a.

Wichmann FA, and Hill NJ. The psychometric function: II. Bootstrap-based confidence intervals and sampling. *Percept Psychophys* 63: 1314-1329, 2001b.